ChemComm

Accepted Manuscript

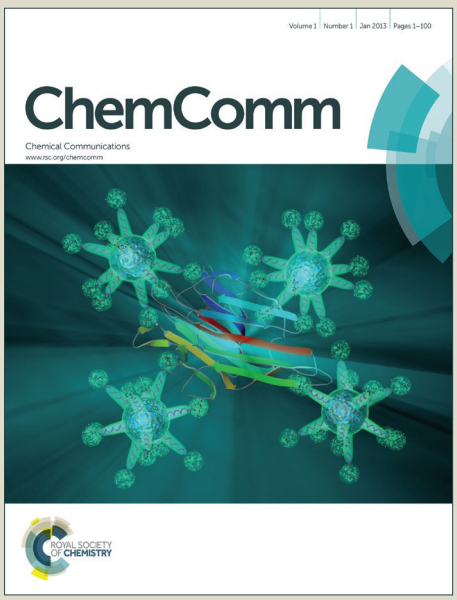

ROYAL SOCIETY OF CHEMISTRY

www.rsc.org/chemcomm

ChemCommun.

COMMUNICATION

Paper-Supported Graphene-Ionic Liquids Array for E-nose Application

Received 00th January 20xx,
Accepted 00th January 20xx

DOI: 10.1039/x0xx00000x

www.rsc.org/

X. Zhu[a], D. Liu[a], Q. Chen [a], L. Lin[a], S. Jiang[a], H. Zhou[a], J. Zhao[b], J. Wu[a]*

A flexible graphene sensor array has been fabricated by in-situ reduction of graphene oxide (GO) array patterned on a paper chip. To achieve the cross-reactive sensing and gas discrimination ability, the surface of each reduced GO (rGO) spot was modified with different types of ionic liquids (ILs), which can significantly alter the semiconductor property and consequently the gas sensing behaviour of the paper-supported rGO sensor.

Gas sensors based on nanomaterial such as gold nanocluster[1] and carbon nanomaterials[2]offer significant advantages over conventional metal oxide-based gas sensor[3] in terms of sensitivity, selectivity, and room-temperature operability. Graphene has emerged as an superior electronic material with exceptional thermal, mechanical, and electrical properties because of its two-dimensional sp^2 carbon bonded structure[4]. Moreover, the band gap of graphene can be modulated by the chemically doppingor surface modification[5,6]. For example, pristine graphene displayed a semi-metallic property with near zero band gap, while a hydrogenated graphene displayed semiconductor characteristics with energy gap of 3.5 eV.[7] P-type doping of epitaxial graphene (EG) has been achieved by surface modification with the molecular electron acceptor[8]. Therefore, the ability to introduce a band gap in graphene with a simple and reproducible manner will facilitate the fabrication of graphene-based devices. Theoretical studies have predicted that the conduction of the graphene channel can be tuned by adsorption of gas molecules[5,6], leading to the sensitive response towards gase molecules[9]. This pioneering work inspired numerous researches on graphene-based gas sensors. Among them, reduced graphene oxide (rGO) have been extensively used as sensing material mainly due to the fact that it can be produced on a large scale at a relatively low cost[10]. In addition, the residual oxygenated group facilitates rGO sheets for chemical modifications[11]. Unfortunately, pristine rGO has exhibited low sensitivity and irreversibility towards gases probably due to its narrow band gap. To overcome this problem, novel nanostructured graphene such as steam etched porous GO[12] , polycrystalline graphene ribbons[13],macroscopic three-dimensional graphene foam networks[14], rGO conjugated Cu_2O nanowire mesocrystals[15], carbon nanotube/graphene hybrid films, and surface modified rGO[16] have been prepared to improve the performance of graphene-based gas sensors. Among different technologies mentioned above, surface modification is the simplest way to harness the band gap of graphene. Herein, we report a flexible chemiresistive gas sensor array constructed from paper supported rGO whose surface was modified with different types of ionic liquids (ILs). The tunable chemical structures of IL provide great possibility to design a graphene-based e-nose with gas discrimination ability. Furthermore, we found that ILs changed the semiconductor properties of rGO, leading to the reversion of intra-sheet resistance response. The sensing array produce a characteristic responding pattern to both inorganic gases and volatile organic compounds (VOCs), leading to the successful gas discrimination. Such a flexible, low-cost graphene-based e-nose will find practical application in portable and wearable sensing device.

The morphologies characterization (Fig. S1, ESI) indicated that the thickness of the purchased GO is around 0.55 ~1.2 nm. Accordingly, the numer of GO layer is estimated to be less than 3. The size distribution of GO sheet range from 0.5 to 3 μm. The process for preparing IL-rGO sensing array is illustrated in Scheme 1. First, the sensing array was pattern on a filter paper using wax printing to create a circle hydrophobic barrier. Then, around 500 μL of GO sol(2mg/ml) was filtered through each of the circle area. Afterwards, the GO retained on the cellulose network was reduced by hydrazine hydrate steam at 90℃ for 3 hours. Finally, The surface of rGO on different sensing spot was then modified with different types of ionic liquids (ILs) by filtering different types of ILs/acetonitrile solution through each circle area. The residue acetonitrile solvent was vaporized in room temperature. Scan electron microscopy (SEM) images

[a] *Institute of Microanalytical System, Department of Chemistry, Zhejiang University, Hangzhou, 310058, China.*
[b] *Wuxi entry exit inspection n and Quarantine Bureau, Wuxi, 214101, China.*
[c]

Electronic Supplementary Information (ESI) available: [details of any supplementary information available should be included here]. See DOI: 10.1039/x0xx00000x

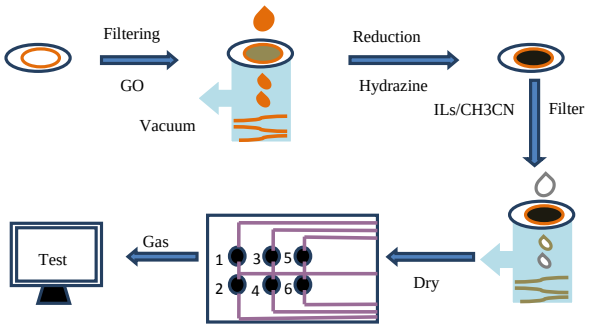

Scheme 1.The procedure for the preparation of paper supported rGO-IL sensor array.

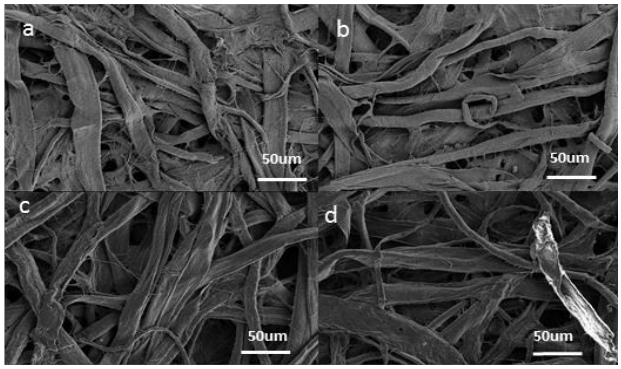

Figure 1.SEM image of a) blank filter paper; b) filter paper loaded with GO; c) paper supported rGO formed by in-situ reduction of GO; d) the rGO paper chip modified with $BmimBF_4$.

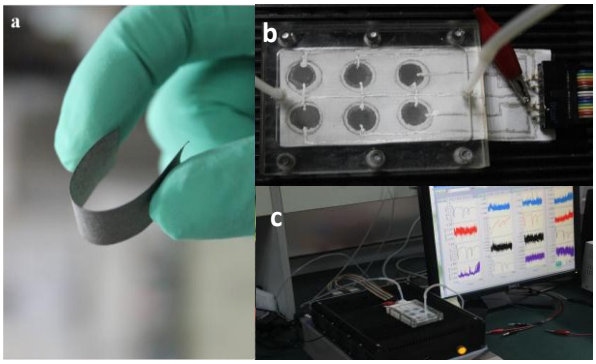

Figure 2.*a) A flexible paper-supported rGO-IL chip; b) The paper-supported rGO-ILs sensor array clamped in a PMMA gas flow chamber; c) The whole e–nose system for gas detection and discrimination.*

show that the morphology of fiber network adsorbed with GO is almost the same as that of blank paper chip (Fig. 1a, b), indicating that a thin layer of GO sheet tightly stick on the surface of cellulose fiber without changing the morphology of fiber network. Before SEM measurement, both blank paper and GO loaded paper need to be sputtered with gold layer, because both samples were non-conductive material. After exposing the GO paper in hydrazine vapor, the brown color of GO turned to gray, indicating the reduction of GO to rGO. Without gold sputtering, a clear SEM image was observed on the rGO loaded paper owing to its good conductivity(Fig. 1c). After the adsorption of ILs, the porous structure of fiber network still remained (Fig. 1d). Such a structure will faciliate the fast gas diffusion and consequently produce rapid response. Raman spectra of GO sample displayed two characteristic peaks of D and G, whose intensity ratio (I_D/I_G) increased after reduction (Fig. S2, ESI), implying that the disorder of carbon atoms increased. Usually, the reduction process can reduce the size of graphene sheet, causing the increasing of edges and defects[17]. The surface chemistry of graphene loaded paper were characterized with X-ray photoelectron spectrometer (XPS). Compared with GO loaded sample (Fig. S3a, ESI), the oxygen peak (O1s, 532.67eV) found on the rGO sample decreased significantly, which is an indicative of partial reduction of the rGO sample (Fig. S3b, ESI). After the rGO was adsorbed with $BmimBF_4$, the peak of elemental fluoride (F1s, 688.78eV) was observed, confirming the successful adsorption of IL on rGO surface (Fig. 3Sc, ESI).The adsorption of the IL on the rGO paper was also proved by UV spectra (Fig. S4, ESI).

The filter paper still kept its flexible property after several steps of treatment (Fig.2a). The flexibility is a demanded characteristic for a wearable sensing device, although we did not use this property in current work. To construct a gas sensing device, the paper chip comprising six sensing spots was connected with silver-based conductive circuit (Fig.2b). For gas detection, the paper chip was clamped in a PMMA gas flow chamber. The resistance change of each sensing spot was monitored with a multichannel conductance measuring device (Fig. 2c). The resistance response of rGO and rGO-IL sensing spot towards air sample, NO_2, Cl_2 and toluene was tested, respectively. We found rGO and rGO-IL sensors showed remarkable different responding behavior towards gas samples. For examples, the rGO sensor almost didn't respond to air sample and toluene vapor, but displayed a positive current response to NO_2 and Cl_2 gas. In contrast, the rGO-$BmimBF_4$ sensor produced a negative conductance response towards the four kinds of gas sample (Fig. 3). Moreover, a fast and reversible conductance response was observed on the rGO-$BmimBF_4$ sensor. Compared with the blank rGO sensor, the sensitivity of rGO-$BmimBF_4$ apparently increased. Factors affecting the sensitivity of rGO and rGO-ILs were investigated as well. Smaller response was found on the paper chip loaded with lower amount of rGO, probably owing to the low coverage of rGO on the filter paper. With the increasing of rGO content, the sensitivity significantly increased and then become stable after the concentration of GO sol exceeds 1.5 $mg{\cdot}mL^{-1}$(Fig. S5, ESI). The duration for GO reduction did not exert significant impact on the sensitivity of rGO paper chip, when the reduction time exceeded 1 hr (Fig. S6, ESI).

In order to further explore the influence of ionic liquids on the sensing behavior of the rGO-ILs, the amount of ILs for surface modification was adjusted by passing different concentration of $BmimBF_4$/acetonitrile (MeCN) solution through the rGO paper chip. The results indicated that the content of IL adsorbed on rGO imposed a remarkable effect on the conductance response of the sensing material (Fig. S7, ESI). The sensor produced a positive conductance response to Cl_2,

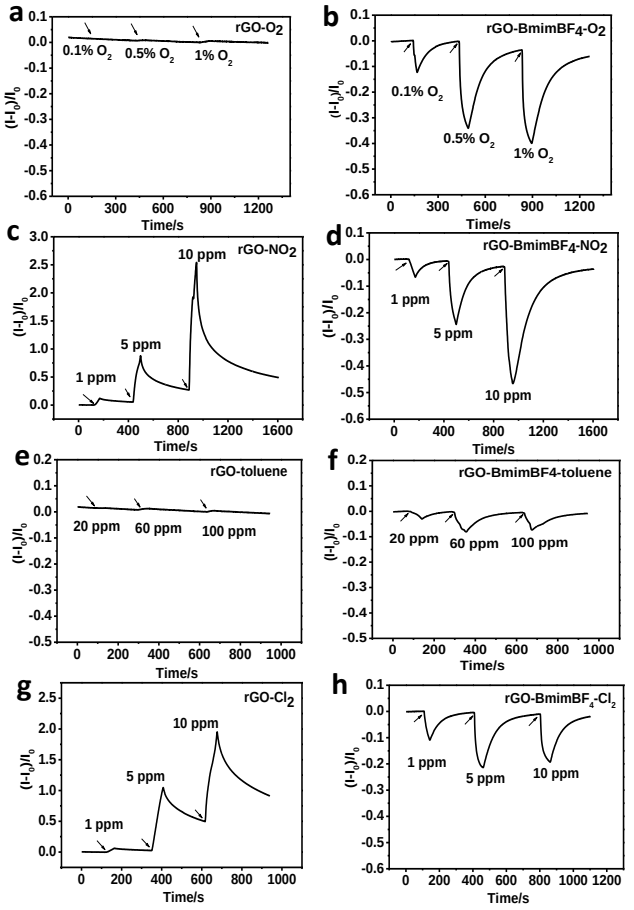

Figure 3.The conductance response of paper-supported rGO chip to a) diluted air sample containing 0.1%~1.0% O_2; c) NO_2 (1~ 10 ppm); e) Toluene vapor (20~100 ppm); g) Cl_2 (1~ 10 ppm). The resistance response of the paper supported rGO-$BmimBF_4$ chip to b) diluted air sample containing 0.1%~1.0% O_2; d) NO_2 (1~ 10 ppm); f) Toluene vapor (20~100 ppm); h) Cl_2 (1~ 10 ppm).

when the ratio of $BmimBF_4$ to MeCN was below than 60:1000 (*v/v*). On contrary, a negative current response was observed when the ratio of IL to MeCN exceeded 100:1000. Therefore, we can speculate that the sensing mechanism of rGO modified with different amount of IL should be different. As shown in the XPS characterization, the rGO sample still contains oxygen groups. This oxygen doped graphene exhibits p-type semiconductor characteristics[11]. Adsorption of strong electron-withdrawing gases (eg. NO_2, Cl_2) will increase the hole density of rGO, thereby increase the conductance of the sensing material according to the intra-sheet mechanism (Fig. 3c, 3g). After the surface modification, the sensing behavior turns to that of n-type semiconductor, which has a negative conductance response to electron-withdrawing gas. We hypothesized that imidazolium group, the cationic part of IL, may donate their electron to the rGO sheet, leading to the conversion of semiconductor properties from p-type to n-type. To confirm this speculation, Hall Effect of the chip was measured on a nanometrics HL5500 hall system. The results showed that the carrier concentration of the rGO and rGO-$BmimBF_4$ paper chip was $+2.929e^{+17}cm^{-3}$ and $-1.039e^{+16}cm^{-3}$, respectively. The positive value is an indicative of p-type semiconductor property, whereas the negative value is corresponding to n-type semiconductor. The rGO-ILs with low content of IL still displayed p-type semiconductor behavior in response to Cl_2 (Fig. S7, ESI), because the p-type property dominated the sensing material, whose surface coverage occupied by IL was in low range. In contrast, after the ratio of IL to rGO exceed a critical value (eg. 100:1000), the n-type property dominate the rGO-ILs composite, leading to the reversion of resistance response (Fig. S7, ESI). However, the negative response decreased when extra amount of ILs located on the sensing material. The mechanism has not been fully understood, but we can assume that the ionic conductivity of ILs may govern the overall conductivity when excess amount of IL existed in the system. The sensing behavior of rGO-ILs towards volatile organic compounds (VOCs) should be ascribed to the inter-sheet effect. IL intercalating between the spaces of rGO sheets may affected on the electron hopping ability between adjacent sheets. Our previous work have proved that, upon exposing to VOCs, the viscosity of the ILs located in nano-confined space remarkably decreased, thereby causing the volume expansion of ILs[18]. In the present case, the volume expansion of ILs will lead to the increase of distance between the adjacent rGO sheets, thereby decrease the conductance of rGO-IL (Scheme S1, ESI). To confirm this assumption, three types of VOC sample were tested on rGO-$BmimPF_6$ chip and rGO-$N_{6,2,2,2}NTf_2$ chip, respectively. Each kind of VOC sample produces negative conductance response on both rGO-IL chips (Fig. S8, ESI). Therefore, the results are complied with the inter-sheet mechanism.

Gas recognition and discrimination is still a challenge in sensor research. Graphene-based sensor has never been reported to have the ability of gas recognition owing to the lack of diverse surface chemistry. As a proof-of-concept work, five kinds of ILs including BmimOTf, $N_{6,2,2,2}NTf_2$, $BmimBF_4$, $BmimClO_4$, $BmimPF_6$ (Table S1, ESI) were selected for the modification of rGO surface. Therefore, the sensor array composes of six sensing elements, along with the blank rGO.. The six sensing elements can generate a unique cross-reactive responding pattern toward a certain kind of gas sample (Fig. S9, ESI, Fig. 4a). Except for the blank rGO, all rGO-IL sensors produce negative but different conductance response to inorganic gases, because different inorganic gas exerts different impact on the charge carrier density of rGO and rGO-IL. In regard to the VOCs (eg. toluene, n-hexane, ethyl acetate), a characteristic cross-reactive responding pattern can be still observed due to the different molecular interaction between ILs and VOC. For example, the anionic part of IL has molecular interaction with polar VOC through dipole-dipole forces; whereas the imidazolium group may has π-π interactions with aromatic VOC. The different molecular interaction between IL and VOC may lead to the different extent of viscosity change and volume expansion[20]. Consequently, the distance between the rGO sheets also changes differently. On the other hand, different gas has its characteristic permittivity (ε_r), which can affect the activation energy of electrons tunneling between different sheets. Therefore, both factors may contribute together to the cross-reactive responding pattern to VOCs on

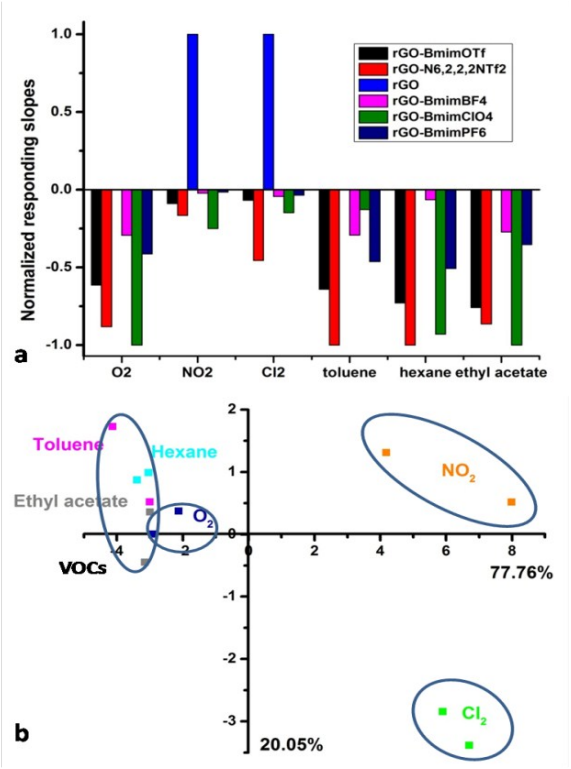

Figure4.a) Comparison of normalized responding slopes among six kinds of gas samples on the paper-supported rGO-IL sensor array; b) Two-dimensional PCA plot obtained from the normalized responding slopes of rGO-IL sensor array in response to six types of gas sample.

the rGO-ILs array. To classify each type of gas samples, principal component analysis (PCA) was employed. After dimension reduction, two main components (PC 1 and PC 2) with variance contribution rate of 77.76% and 20.05% were obtained (Fig. 4b). Each type of inorganic gas obviously separate in different areas, but the VOCs overlap with O_2 gas. However, if the inorganic gases were excluded in the PCA plot, the toluene, ethyl acetate and hexane would be also distinguishable (Fig. S10, ESI). To further evaluate the selectivity of rGO-ILs array, multiple targets detection on the e-nose system were carried out. Parallel detection shows that the data points of toluene-hexane mixture and toluene-ethyl acetate mixture well separate in the PCA plot (Fig. S11, ESI), indicating that the rGO-ILs array is selective to the VOC components in the detection of gas mixture.

Conclusions

In summary, we have constructed a flexible paper-supported rGO-ILs array by a very simple and convenient way. The surface modification of the paper-supported rGO with different types of ionic liquids not only enhanced the sensitivity and reversibility of rGO-ILs sensor, but also imparted the ability of gas recognition due to the different molecular interaction between gas and the selected panel of ILs. Besides, surface modification with ILs significantly altered the semiconductor properties of rGO, leading to the change of gas sensing behavior. Two mechanisms including the intra-sheet and inter-sheet effect successfully explained the unique sensing behavior of the rGO-ILs sensor towards typical inorganic gas and VOCs. The flexible graphene-based e-nose can potentially bring a significant change to our daily life since it was developed on the widely used paper, which can be conveniently pasted onto various substrate and package. If coupled with a wireless signal transmission device, such a flexible e-nose may find application in instant monitoring of air and food quality.

This work was supported by National Science Foundation of China (No.21275218 and 21575127), and Zhejiang Provincial Natural Science Foundation of China (No. Z15B050001)

Notes and references

1 A. W. Snow, M. G. Ancona, D. Park, *Langmuir*, 2012, **28**, 15438.
2 J. Kong, N. R. Franklin, C. W. Zhou, M. G. Chapline, S. Peng, K. J. Cho, H. J. Dai, *Science,* 2000, **287**, 622; S. Majumdar, P. Nag, P. S. Devi, *Mater. Chem. Phys*., 2014, **147**, 79.
3 W. Zeng, T. Liu, Z. Wang, *J. Mater. Chem*., 2012, **22**, 3544; M. Kimura, R. Sakai, S. Sato, T. Fukawa, T. Ikehara, R. Maeda, T. Mihara, *Adv. Funct. Mater*.,2012, **22**, 469.
4 K. S. Novoselov, A. K. Geim, S. V. Morozov, D. Jiang, Y. Zhang, S. V. Dubonos, I. V. Grigorieva, A. A. Firsov, *Science,* 2004, **306**, 666.
5 Y.-H. Zhang, K.-G. Zhou, K.-F. Xie, J. Zeng, H.-L. Zhang, Y. Peng, *Nanotechnology,* 2010, 21, 065201.
6 Y. H. Lu, W. Chen, Y. P. Feng, P. M. He, *J. Phys. Chem*. *B,*2009, **113**, 2-5.
7 J. O. Sofo, A. S. Chaudhari, G. D. Barber, *Phys.Rev. B,*2007, **75**, 153401.
8 W. Chen, S. Chen, D. C. Qi, X. Y. Gao, A. T. S. Wee, *J. Am. Chem. Soc.,*2007, **129**, 10418.
9 F. Schedin, A. K. Geim, S. V. Morozov, E. W. Hill, P. Blake, M. I. Katsnelson, K. S. Novoselov, *Nat. Mater.* 2007, **6**, 652.
10 J. D. Fowler, M. J. Allen, V. C. Tung, Y. Yang, R. B. Kaner, B. H. Weiller, *ACS Nano* 2009, **3**, 301; V. Dua, S. P. Surwade, S. Ammu, S. R. Agnihotra, S. Jain, K. E. Roberts, S. Park, R. S. Ruoff, S. K. Manohar, *Angew. Chem.Int. Ed*. 2010, **49**, 2154
11 Y. Zhou, Y. Jiang, T. Xie, H. Tai, G. Xie, *Sensors and Actuators B: Chemical* 2014, **203**, 135.
12 T. H. Han, Y.-K. Huang, A. T. Tan, V. P. Dravid, J. Huang, *J. Am. Chem. Soc.* 2011, **133**, 15264.
13 A. Salehi‐Khojin, D. Estrada, K. Y. Lin, M. H. Bae, F. Xiong, E. Pop, R. I. Masel, *Adv. Mater.,* 2012, **24**, 53.
14 F. Yavari, Z. Chen, A. V. Thomas, W. Ren, H.-M. Cheng, N. Koratkar, *Sci. Rep.,* 2011, **1**.
15 S. Deng, V. Tjoa, H. M. Fan, H. R. Tan, D. C. Sayle, M. Olivo, S. Mhaisalkar, J. Wei, C. H. Sow, *J. Am. Chem. Soc.* 2012, **13**4, 4905.
16 Y. Lu, B. R. Goldsmith, N. J. Kybert, A. T. C. Johnson, Applied Physics Letters 2010, 97; W.Yuan , A. Liu , L. Huang , C. Li , G. Shi, *Adv. Mater.* 2013, **25**, 766.
17 M. A. Gross, M. J. A. Sales, M. A. G. Soler, M. A. Pereira-da-Silva, M. F. P. da Silva, L. G. Paterno, *RSC Advances* 2014, **4**, 17917.
18 X. Zhu, H. Zhang, J. Wu, *Sens. Actuators B: Chem.,* 2014, **202**, 105-113.
19 E. Dovgolevsky, G. Konvalina, U. Tisch, H. Haick, *J. Phys. Chem. C,*2010, **114**, 14042-14049.
20 K. Ohsawa, H. Takahashi, K. Noda, T. Kan, K. Matsumoto, I. Shimoyama, Ieee, in *2011 Ieee 24th International Conference on Micro Electro Mechanical Systems*, Ieee, New York, 2011, pp. 525